

# Appendix: Rough Sets for Bias Field Correction in MR Images Using Contraharmonic Mean and Quantitative Index

Abhirup Banerjee and Pradipta Maji

**Abstract**—One of the challenging tasks for magnetic resonance (MR) image analysis is to remove the intensity inhomogeneity artifact present in MR images, which often degrades the performance of an automatic image analysis technique. In this regard, the paper presents a novel approach for bias field correction in MR images. It judiciously integrates the merits of rough sets and contraharmonic mean. While the contraharmonic mean is used in low-pass averaging filter to estimate the bias field in multiplicative model, the concept of lower approximation and boundary region of rough sets deals with vagueness and incompleteness in filter structure definition. A theoretical analysis is also presented to justify the use of both rough sets and contraharmonic mean for bias field estimation. The integration enables the algorithm to estimate optimum or near optimum bias field. Some new quantitative indices are introduced to measure intensity inhomogeneity artifact present in a MR image. The performance of the proposed approach, along with a comparison with other intensity inhomogeneity correction algorithms, is demonstrated on a set of simulated MR images for different bias fields and noise levels and a set of real brain MR images.

## I. QUALITATIVE AND QUANTITATIVE EVALUATION

Simulated images with different bias fields (20% and 40%) and noise levels (0%, 1%, 3%, 5%, 7% and 9%) have been generated from “BrainWeb: Simulated Brain Database” and different bias field correction algorithms are applied on them. The results are reported in Fig. 1-12. The proposed algorithm RC2 [1] (rough set (RS) + contraharmonic mean (CHM) filter of order 2) has been compared with the Homomorphic Unsharp Masking (HUM) filtering method [2], [3], nonparametric nonuniform intensity normalization (N3) bias correction method [4] and statistical parameter mapping (SPM8) software tool [5]. The effectiveness of contraharmonic mean (CHM) of order 2 over other measures of central tendency (e.g. arithmetic mean and harmonic mean) is also established. The importance of using rough sets is also shown in the results. Fig. 1-6 shows the results of the images with bias field 20% and different noise levels. Input images with bias field 40% and different noise levels and reconstructed images using different bias field correction algorithms are shown in Fig. 7-12. The root-mean square error (RMSE) values for each of the reconstructed images are also given.

Real T1-weighted brain MR images are downloaded from “IBSR: Internet Brain Segmentation Repository” and different

bias field correction algorithms are applied on them (RC2, RS + AM, RS + HM, NRS + CHM, HUM, N3 and SPM8). The input images along with their reconstructed images using different bias field correction algorithms are shown in Fig. 13-22.

The comparative performance of the proposed algorithm with HUM, N3 and SPM8 over “BrainWeb” database using different quantitative indices (IoV, IoJV, IoCS and RMSE) is shown in Fig. 23 using bar diagrams. Comparison over “IBSR” database is shown in Fig. 24 using IoCS and IoJV indices.

The robustness of the proposed algorithm over different bias field correction algorithms is checked on the unbiased images generated from “BrainWeb: Simulated Brain Database” with different noise levels (0%, 1%, 3%, 5%, 7% and 9%). The performance is analysed using different quantitative indices in Fig. 25 and the results are shown in Fig. 26-31.

## REFERENCES

- [1] A. Banerjee and P. Maji, “Rough Sets for Bias Field Correction in MR Images Using Contraharmonic Mean and Quantitative Index,” *IEEE Transactions on Medical Imaging*, Submitted.
- [2] L. Axel, J. Costantini, and J. Listerud, “Intensity Correction in Surface-Coil MR Imaging,” *American Journal of Roentgenology*, vol. 148, pp. 418–420, 1987.
- [3] B. H. Brinkmann, A. Manduca, and R. A. Robb, “Optimized Homomorphic Unsharp Masking for MR Grayscale Inhomogeneity Correction,” *IEEE Transactions on Medical Imaging*, vol. 17, no. 2, pp. 161–171, 1998.
- [4] J. G. Sled, A. P. Zijdenbos, and A. C. Evans, “A Nonparametric Method for Automatic Correction of Intensity Nonuniformity in MRI Data,” *IEEE Transactions on Medical Imaging*, vol. 17, no. 1, pp. 87–97, 1998.
- [5] J. Ashburner and K. J. Friston, “Unified Segmentation,” *NeuroImage*, vol. 26, no. 3, pp. 839–851, 2005.

The authors are with the Machine Intelligence Unit, Indian Statistical Institute, Kolkata, India. E-mail: {abhirup\_r.pmajj}@isical.ac.in.

This work is partially supported by the Indian National Science Academy, New Delhi (grant no. SP/YSP/68/2012).

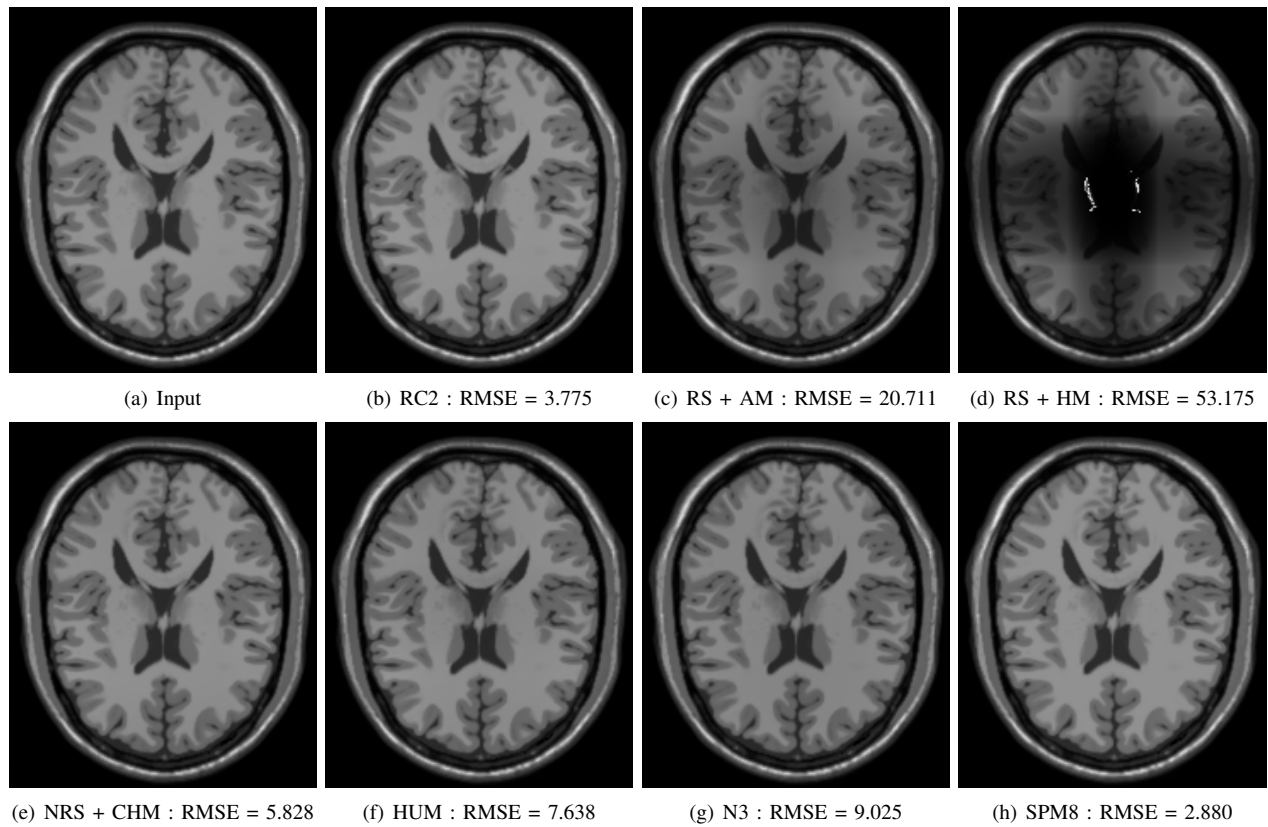


Fig. 1. Image of BrainWeb with 20% bias field and 0% noise and images restored by different algorithms

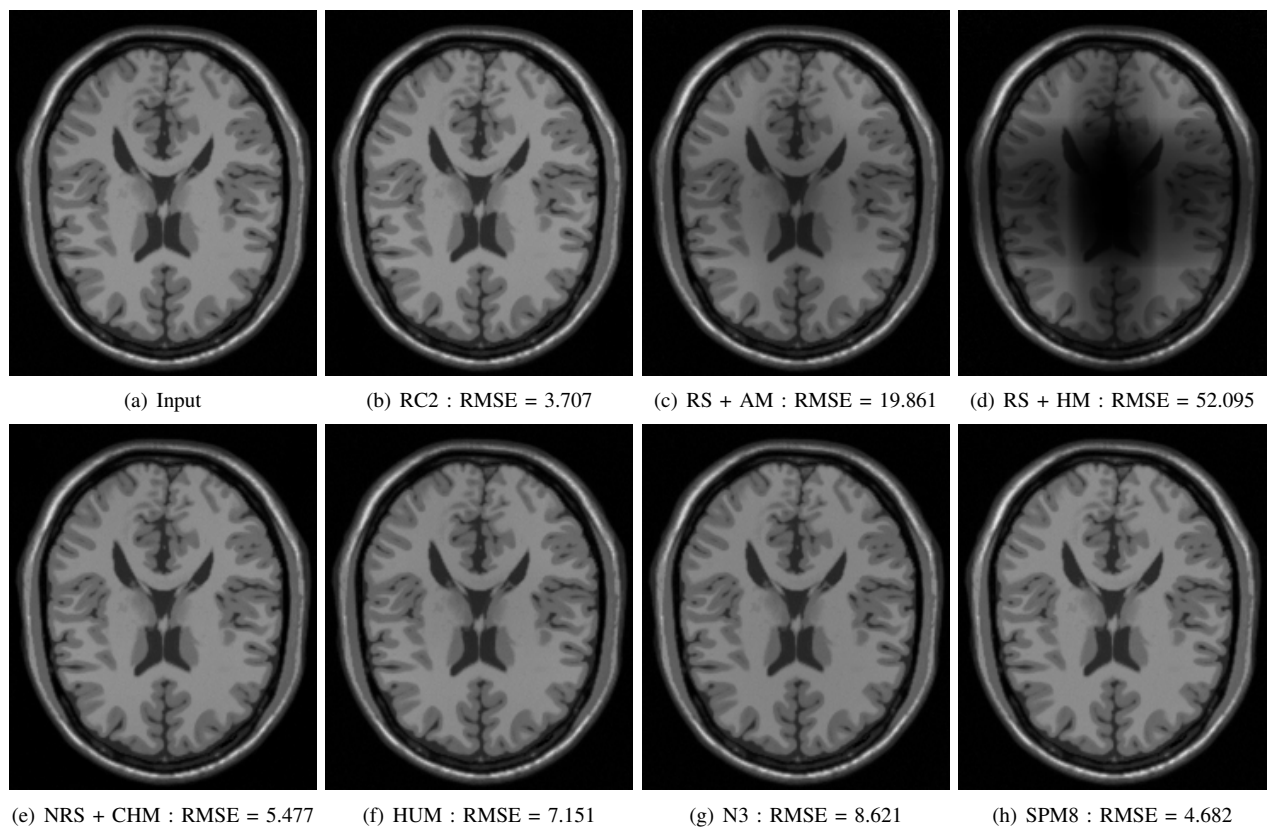


Fig. 2. Image of BrainWeb with 20% bias field and 1% noise and images restored by different algorithms

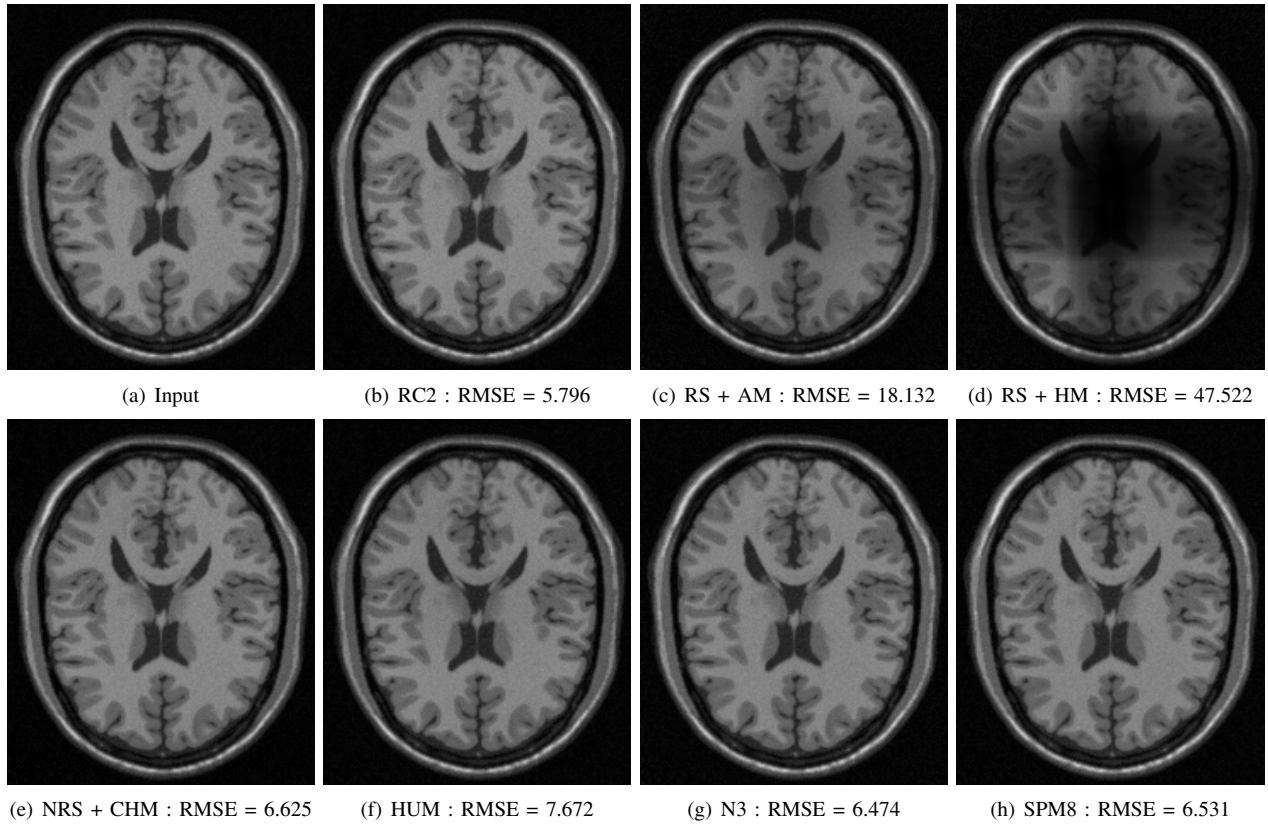


Fig. 3. Image of BrainWeb with 20% bias field and 3% noise and images restored by different algorithms

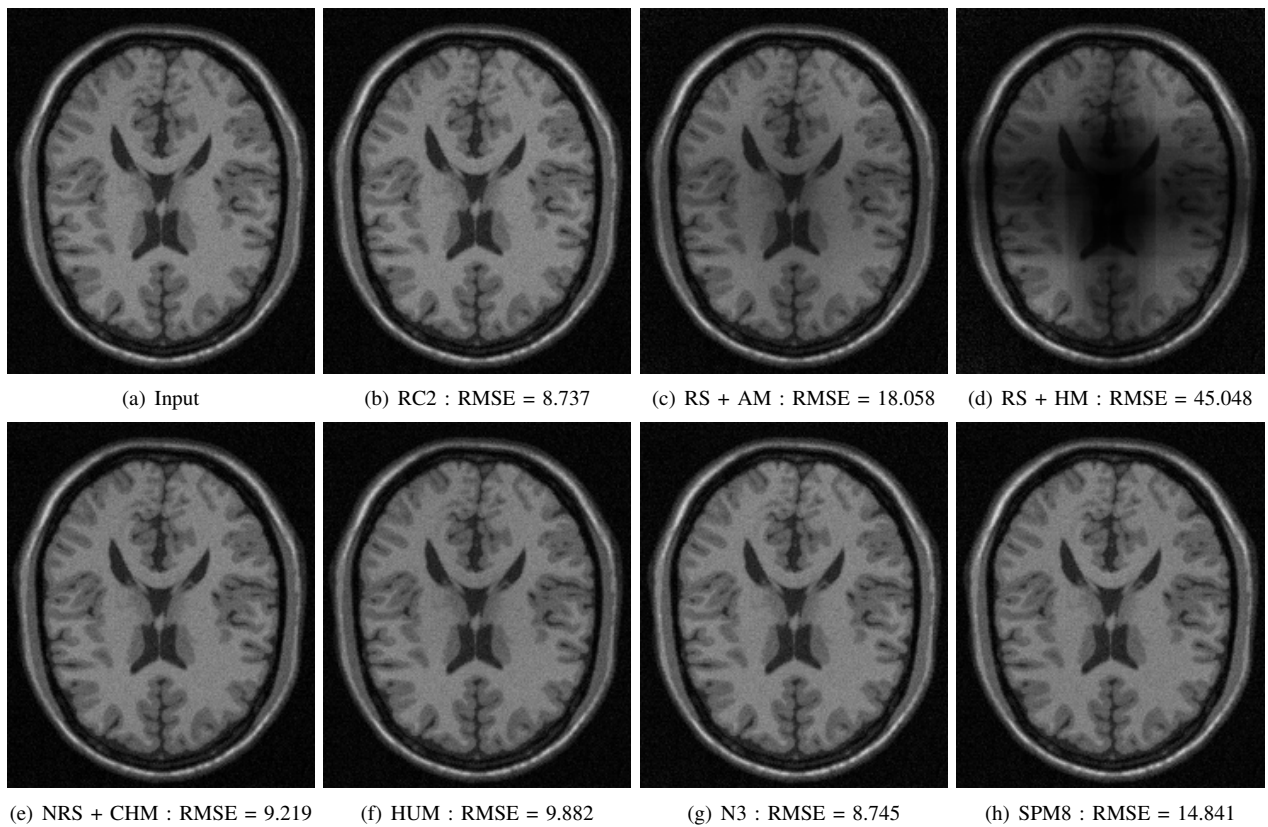


Fig. 4. Image of BrainWeb with 20% bias field and 5% noise and images restored by different algorithms

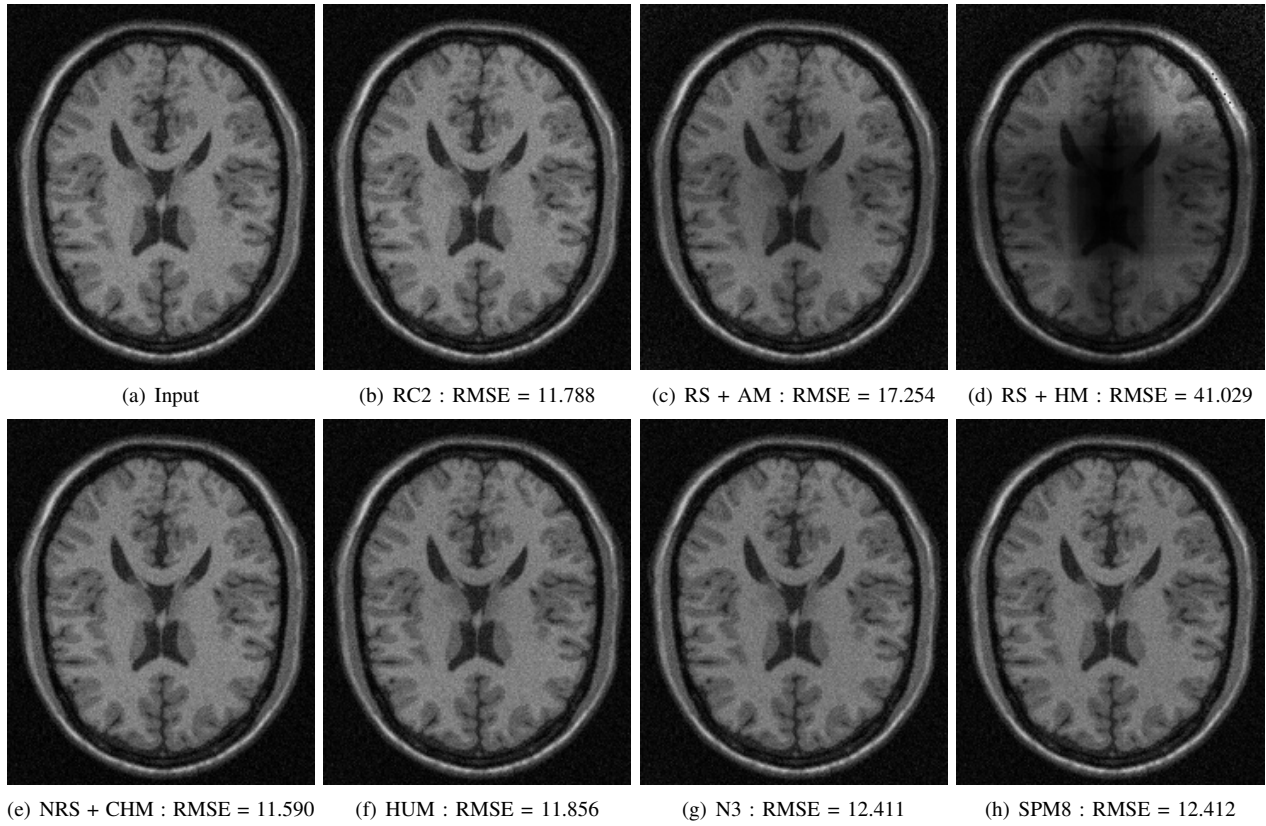


Fig. 5. Image of BrainWeb with 20% bias field and 7% noise and images restored by different algorithms

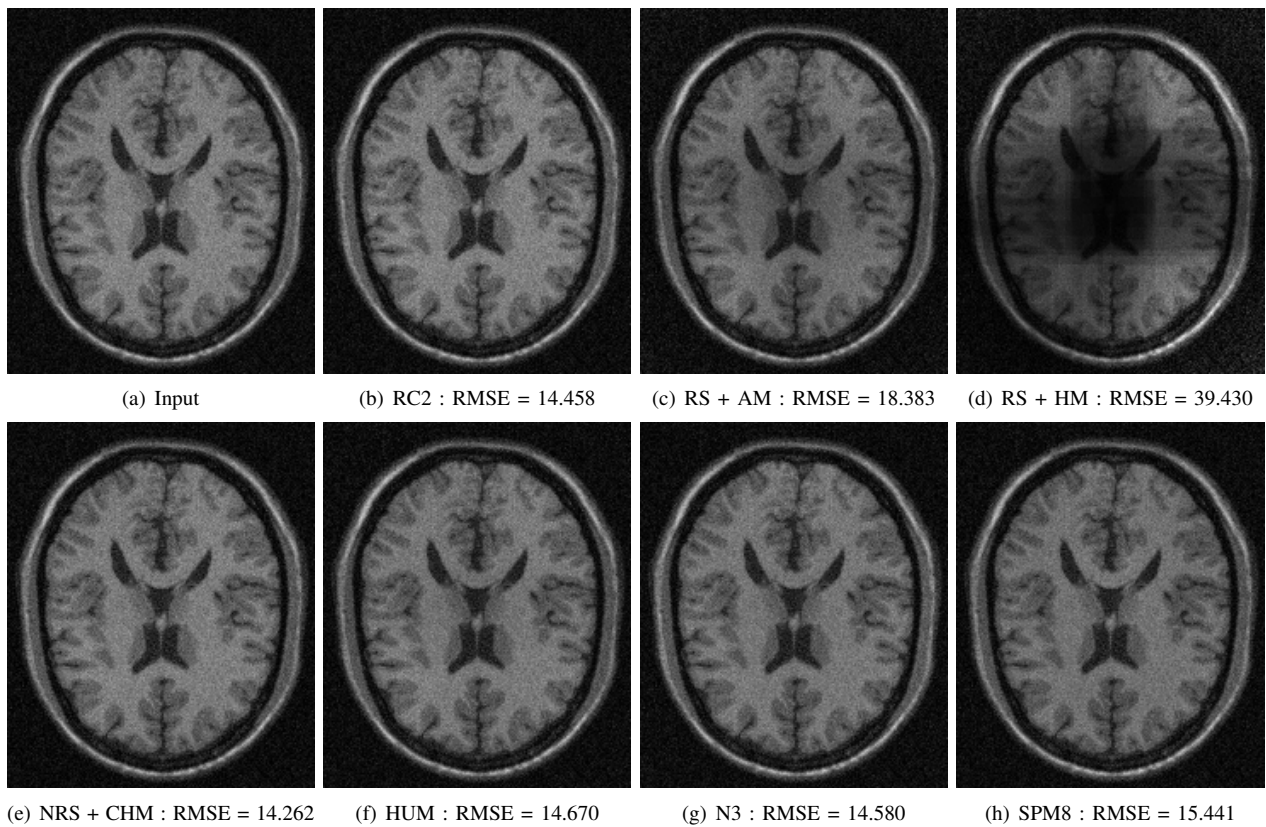


Fig. 6. Image of BrainWeb with 20% bias field and 9% noise and images restored by different algorithms

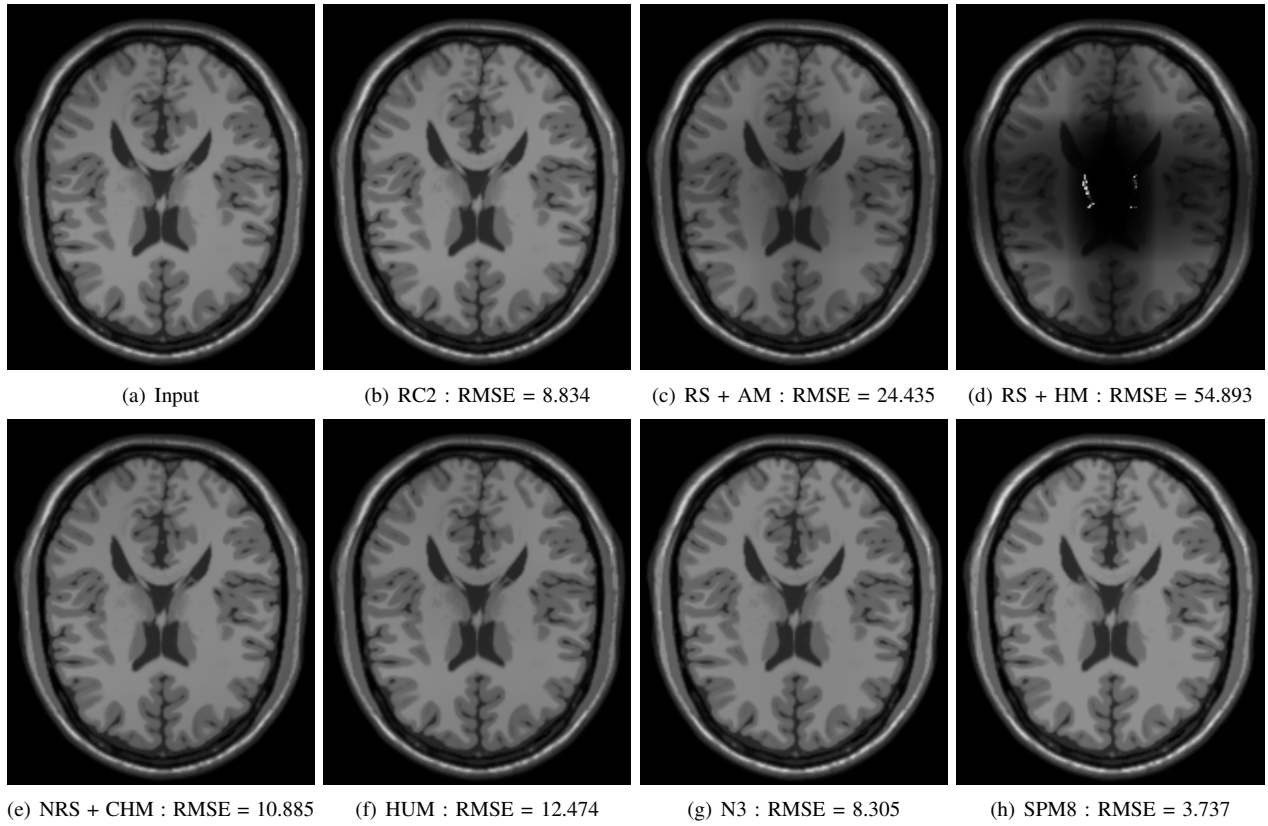


Fig. 7. Image of BrainWeb with 40% bias field and 0% noise and images restored by different algorithms

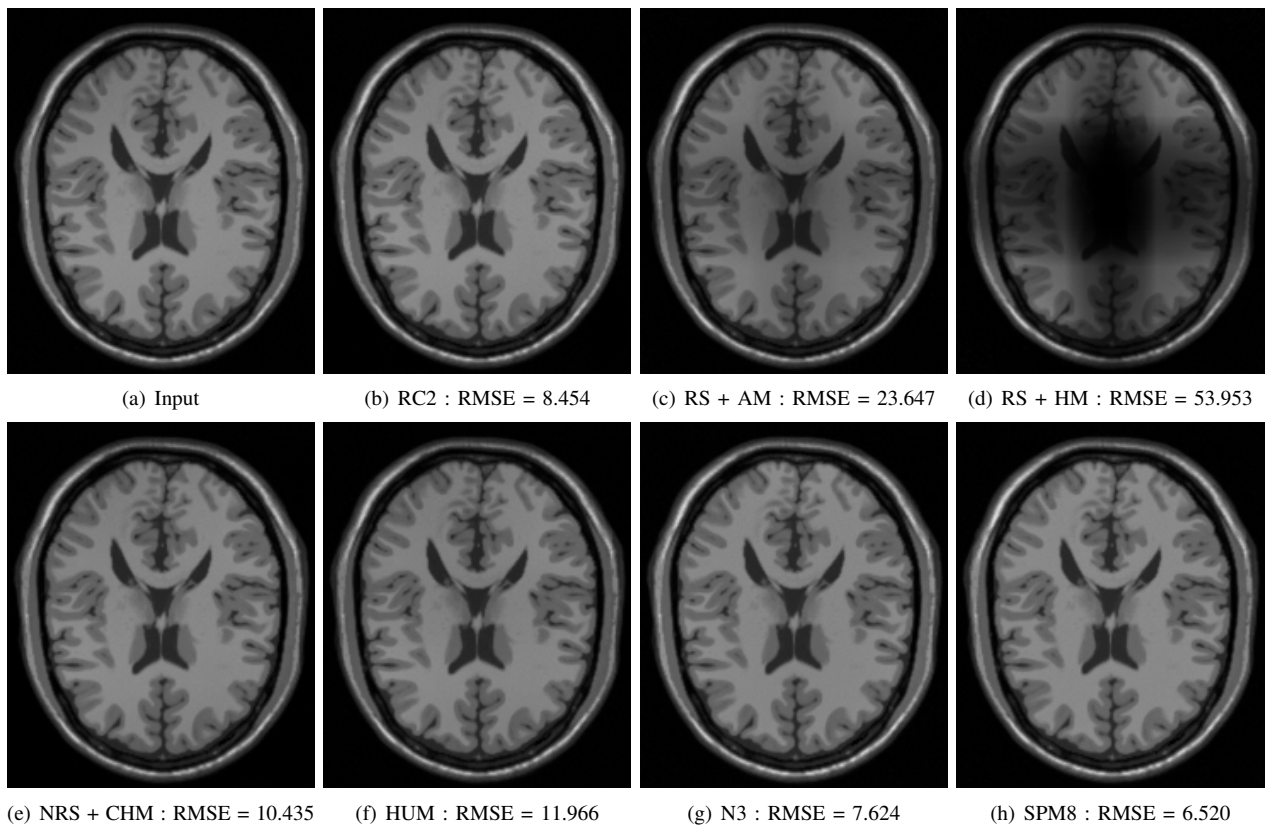


Fig. 8. Image of BrainWeb with 40% bias field and 1% noise and images restored by different algorithms

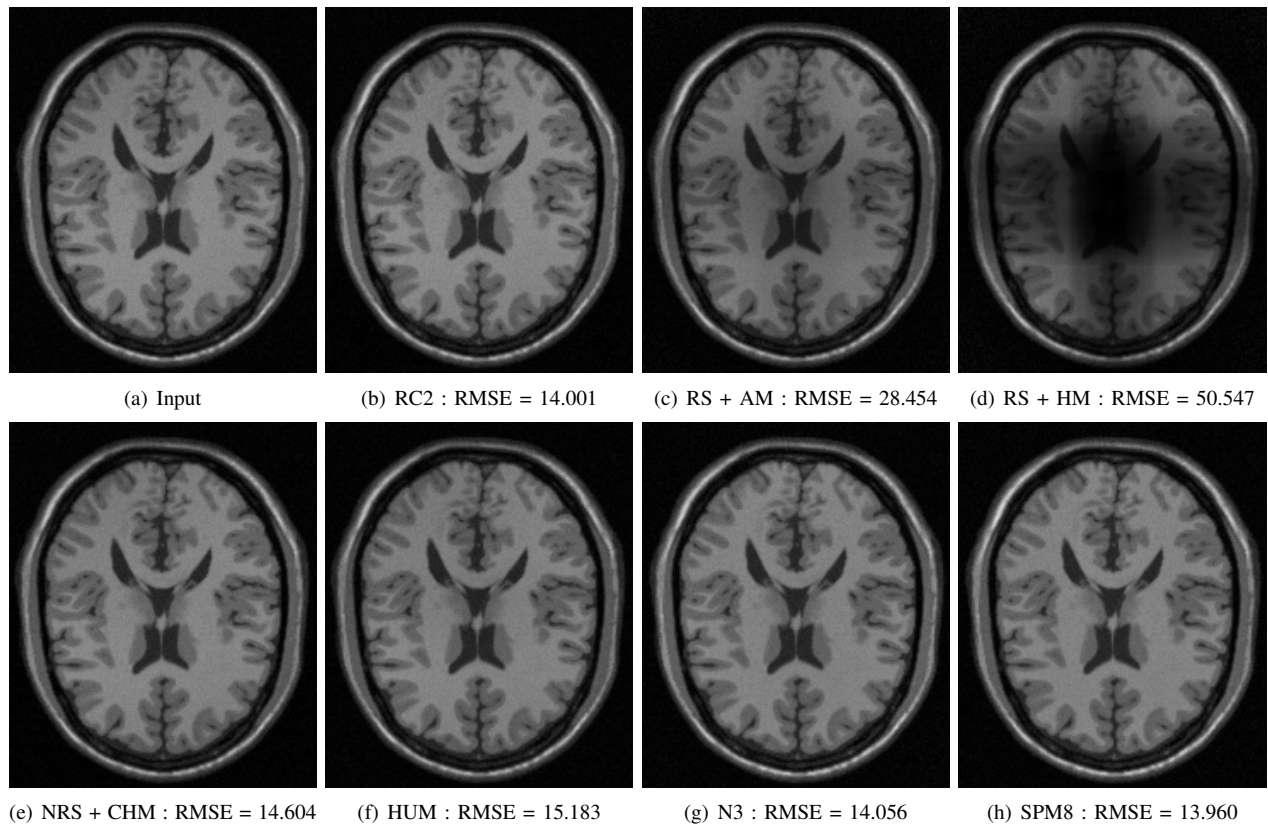


Fig. 9. Image of BrainWeb with 40% bias field and 3% noise and images restored by different algorithms

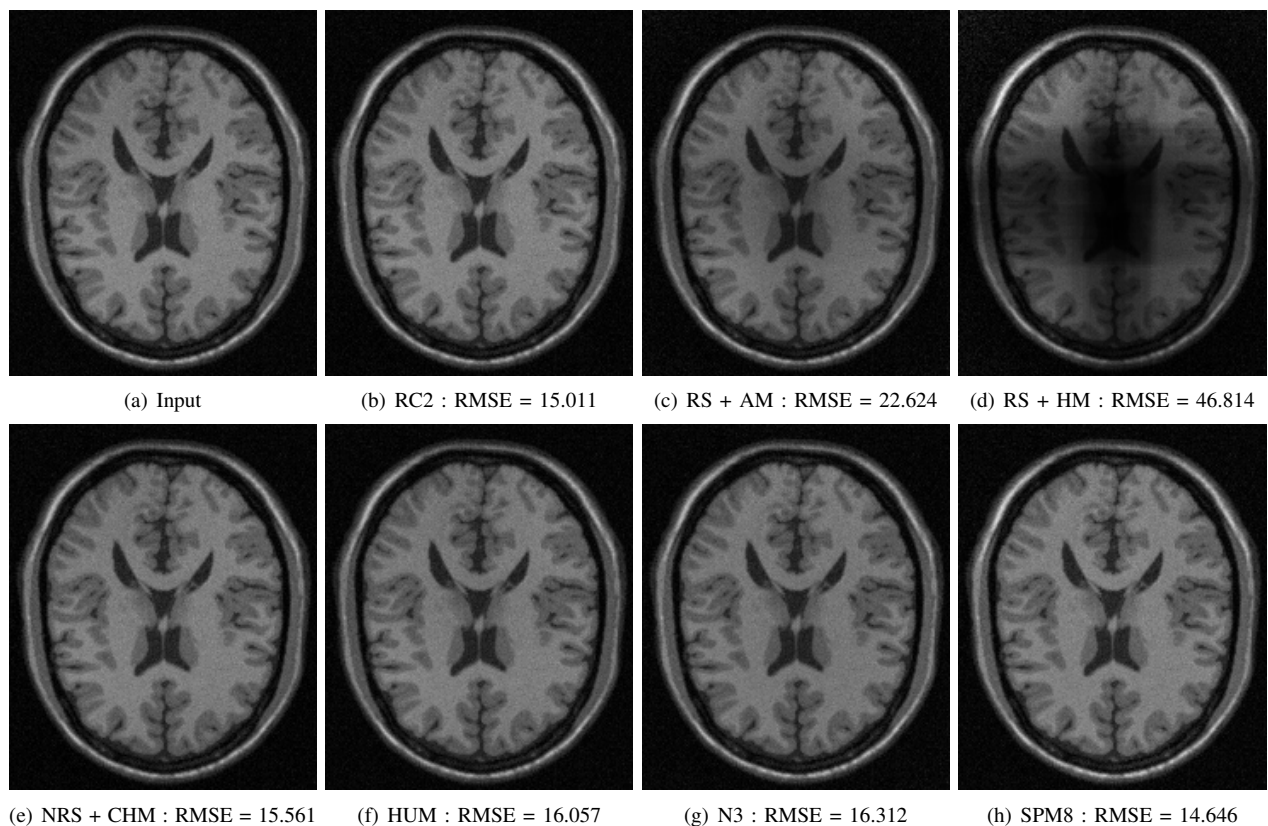


Fig. 10. Image of BrainWeb with 40% bias field and 5% noise and images restored by different algorithms

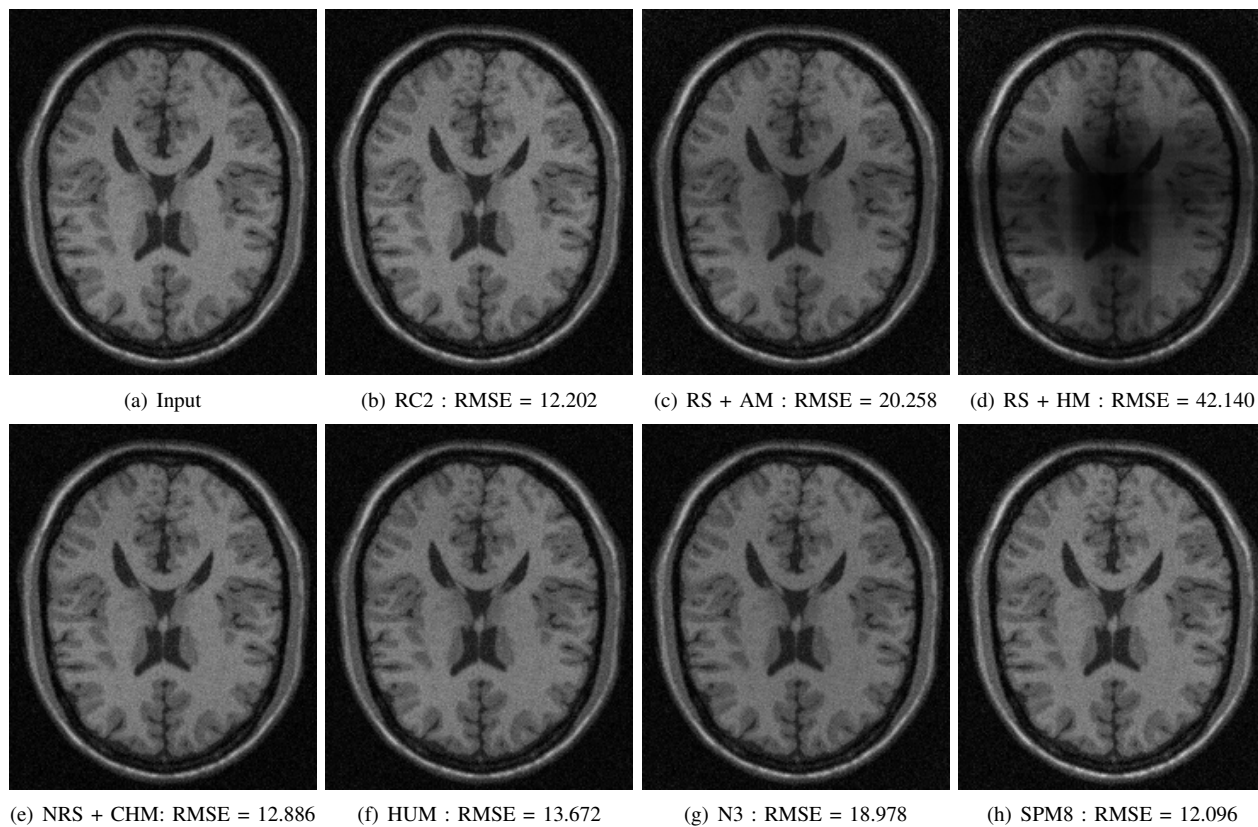


Fig. 11. Image of BrainWeb with 40% bias field and 7% noise and images restored by different algorithms

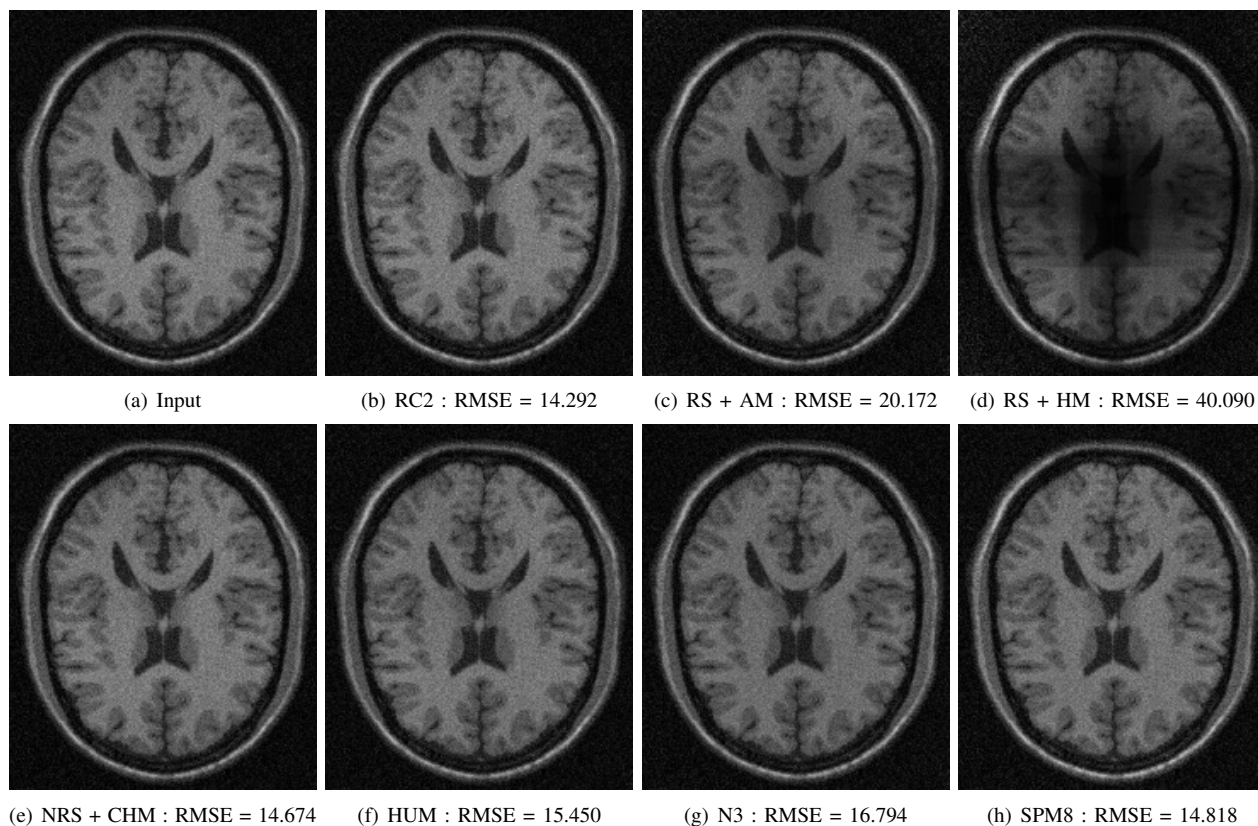


Fig. 12. Image of BrainWeb with 40% bias field and 9% noise and images restored by different algorithms

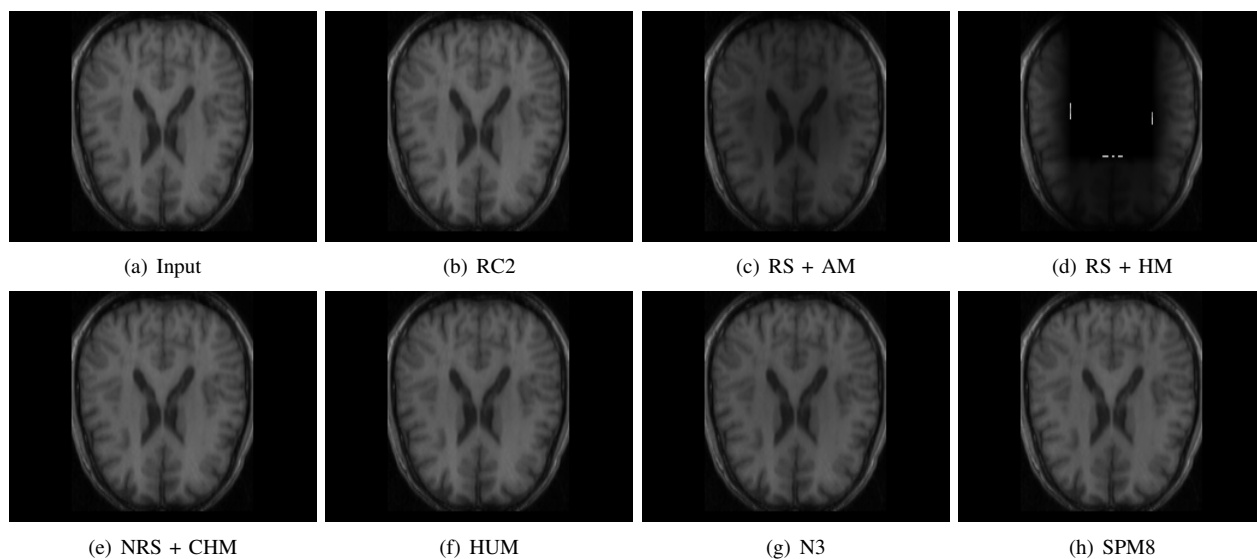


Fig. 13. Real image of IBSR 01 and images restored by different algorithms

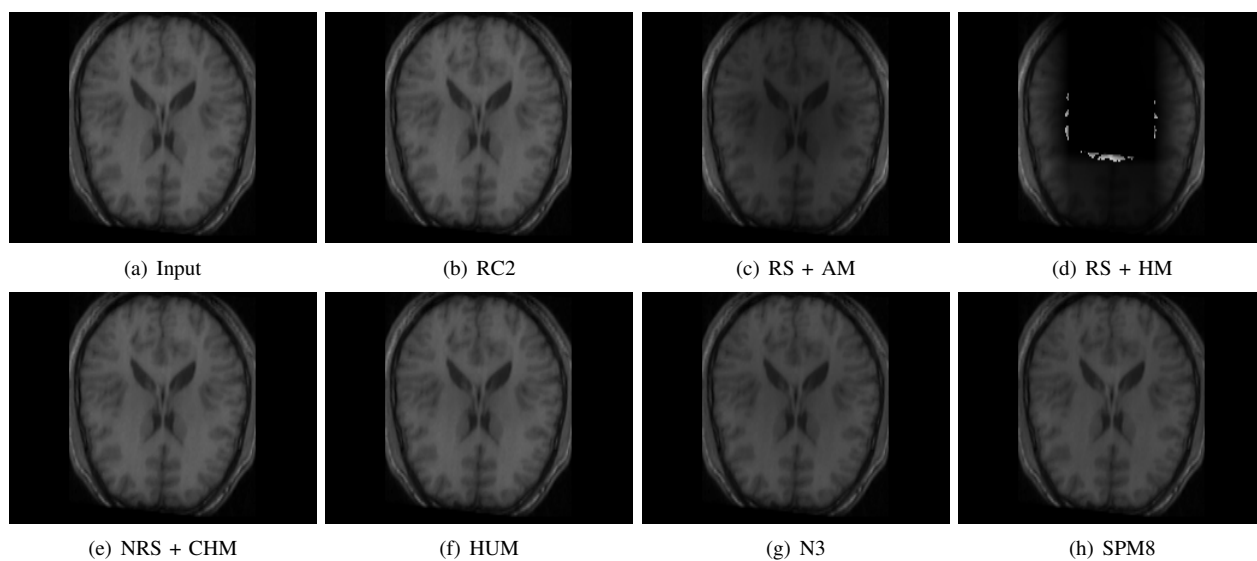


Fig. 14. Real image of IBSR 02 and images restored by different algorithms

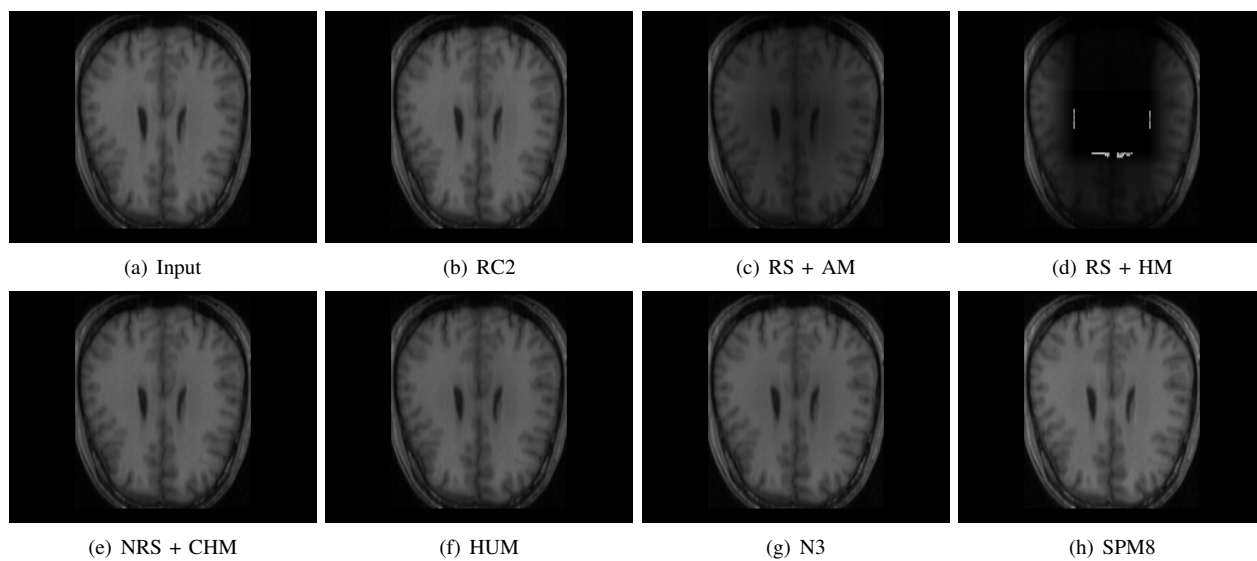


Fig. 15. Real image of IBSR 05 and images restored by different algorithms

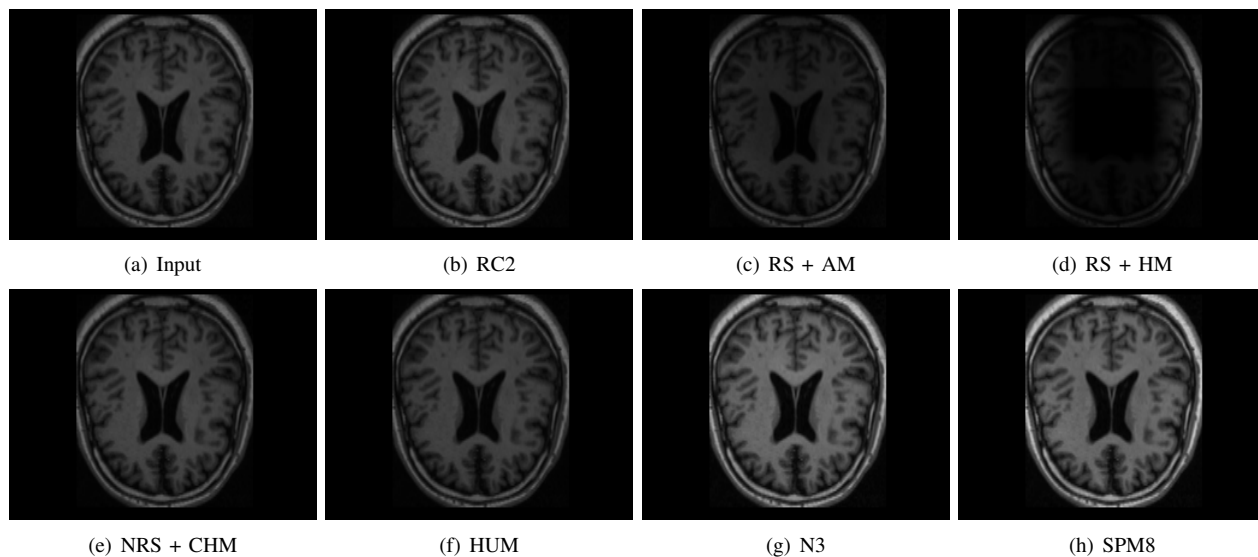


Fig. 16. Real image of IBSR 08 and images restored by different algorithms

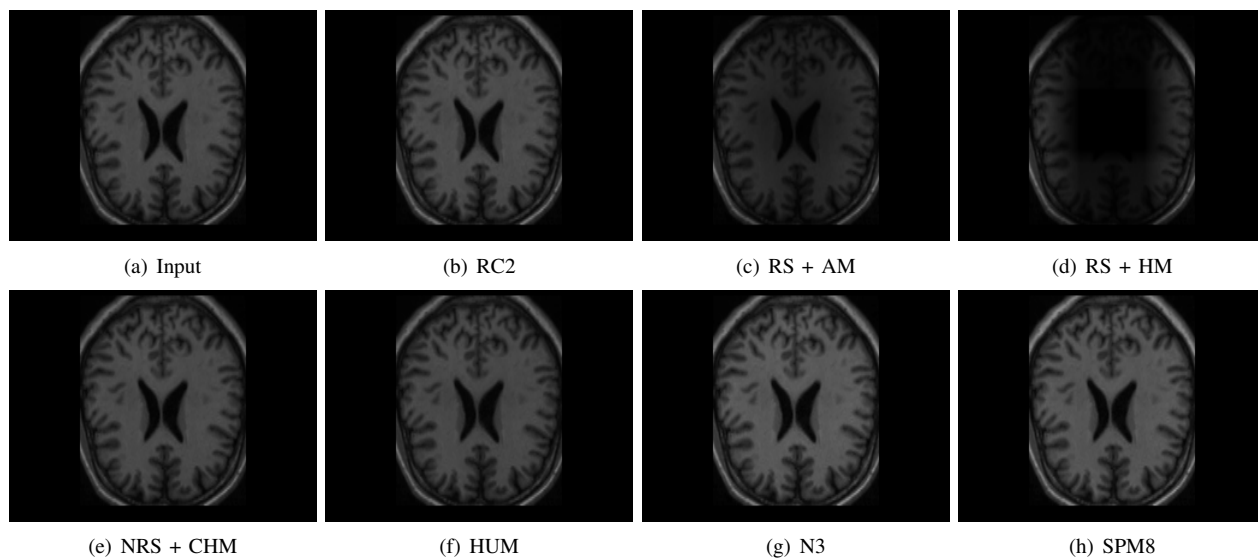


Fig. 17. Real image of IBSR 09 and images restored by different algorithms

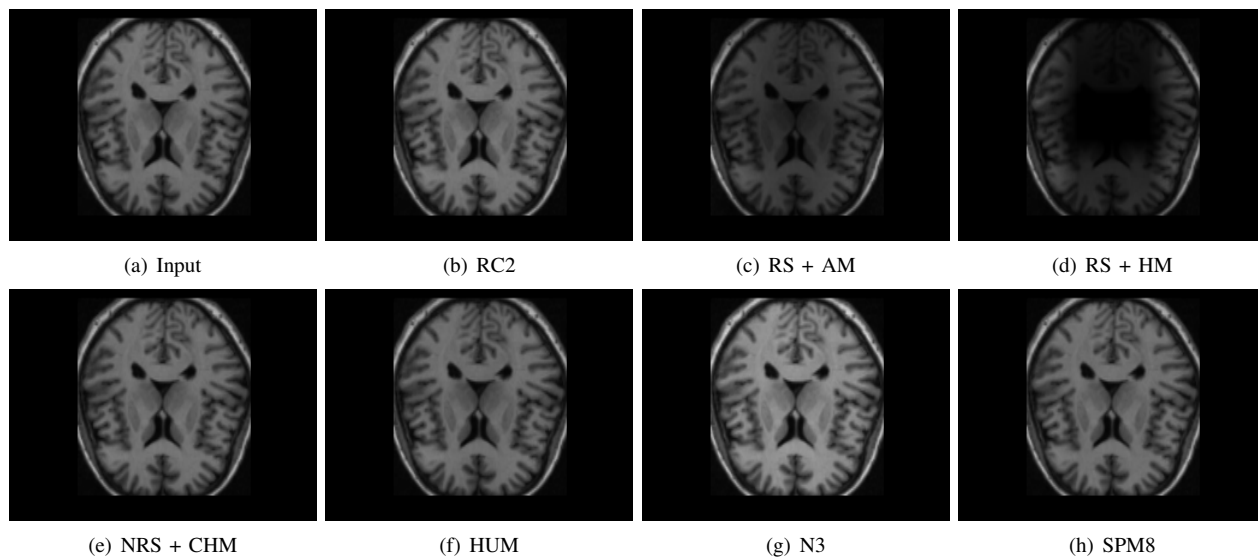


Fig. 18. Real image of IBSR 11 and images restored by different algorithms

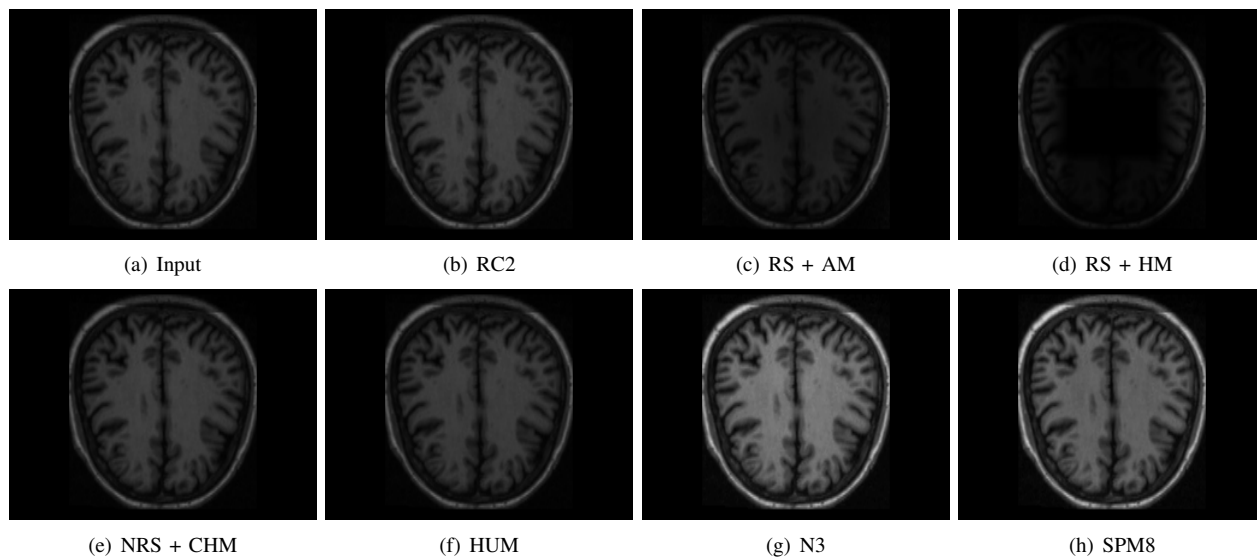


Fig. 19. Real image of IBSR 12 and images restored by different algorithms

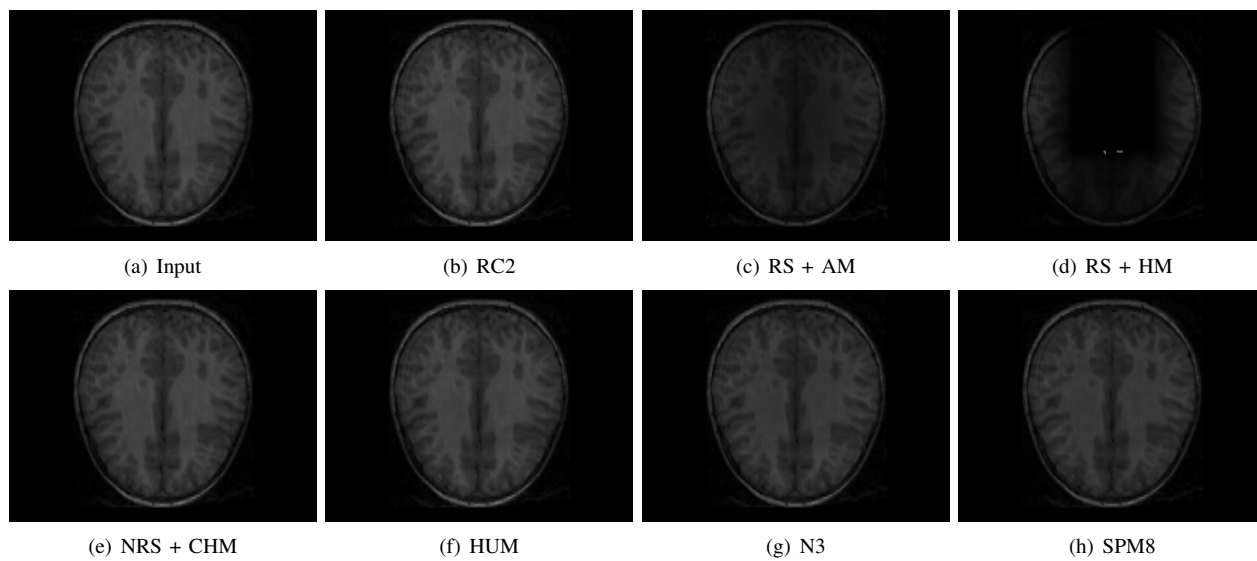


Fig. 20. Real image of IBSR 13 and images restored by different algorithms

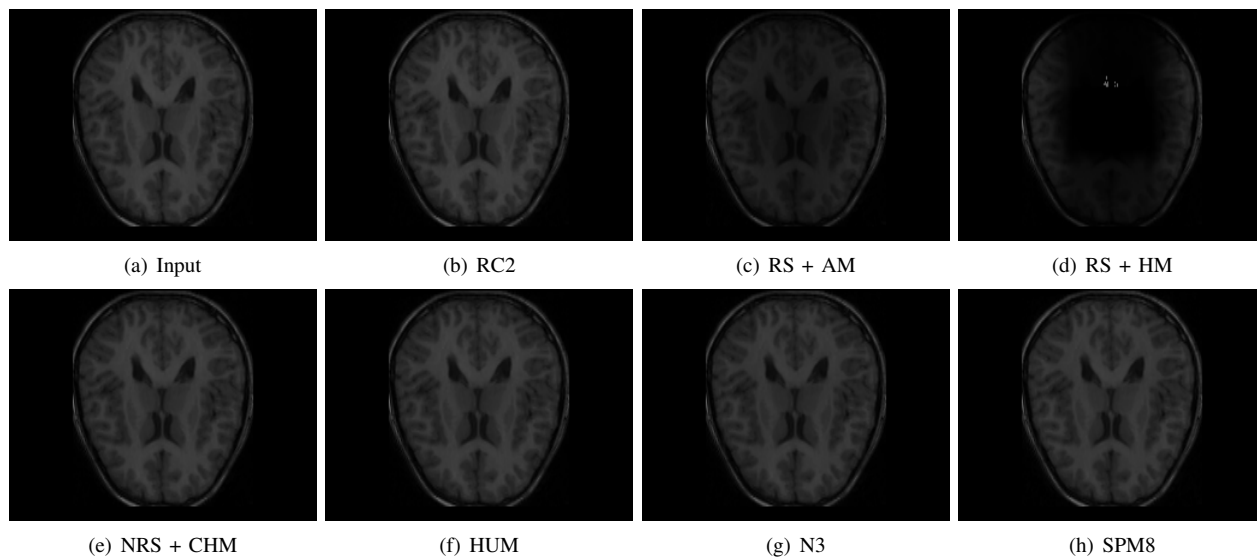


Fig. 21. Real image of IBSR 14 and images restored by different algorithms

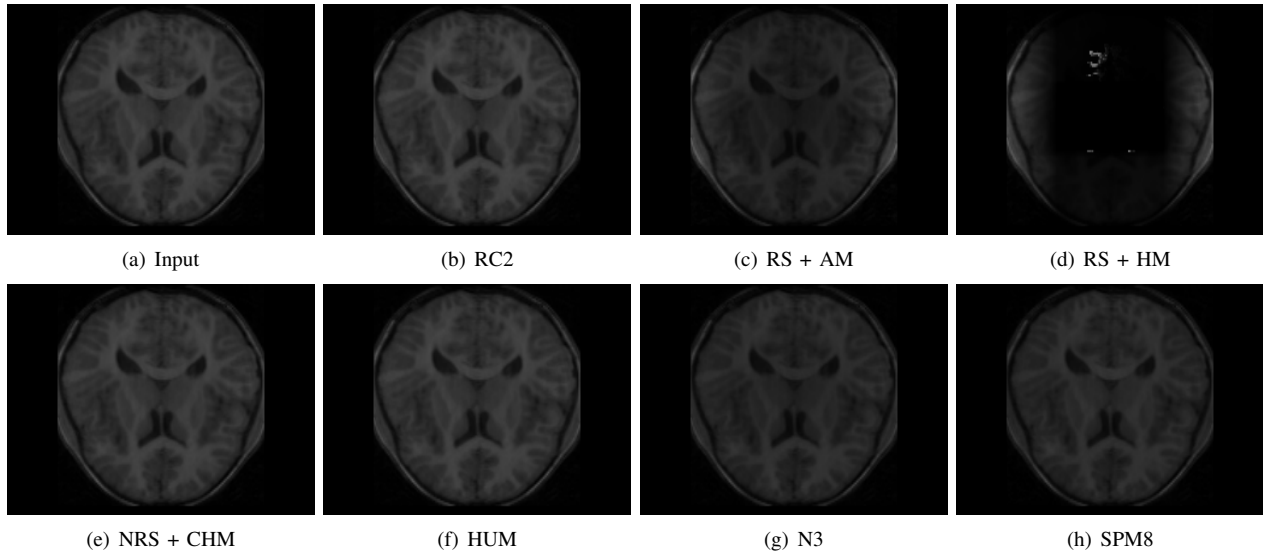


Fig. 22. Real image of IBSR 17 and images restored by different algorithms

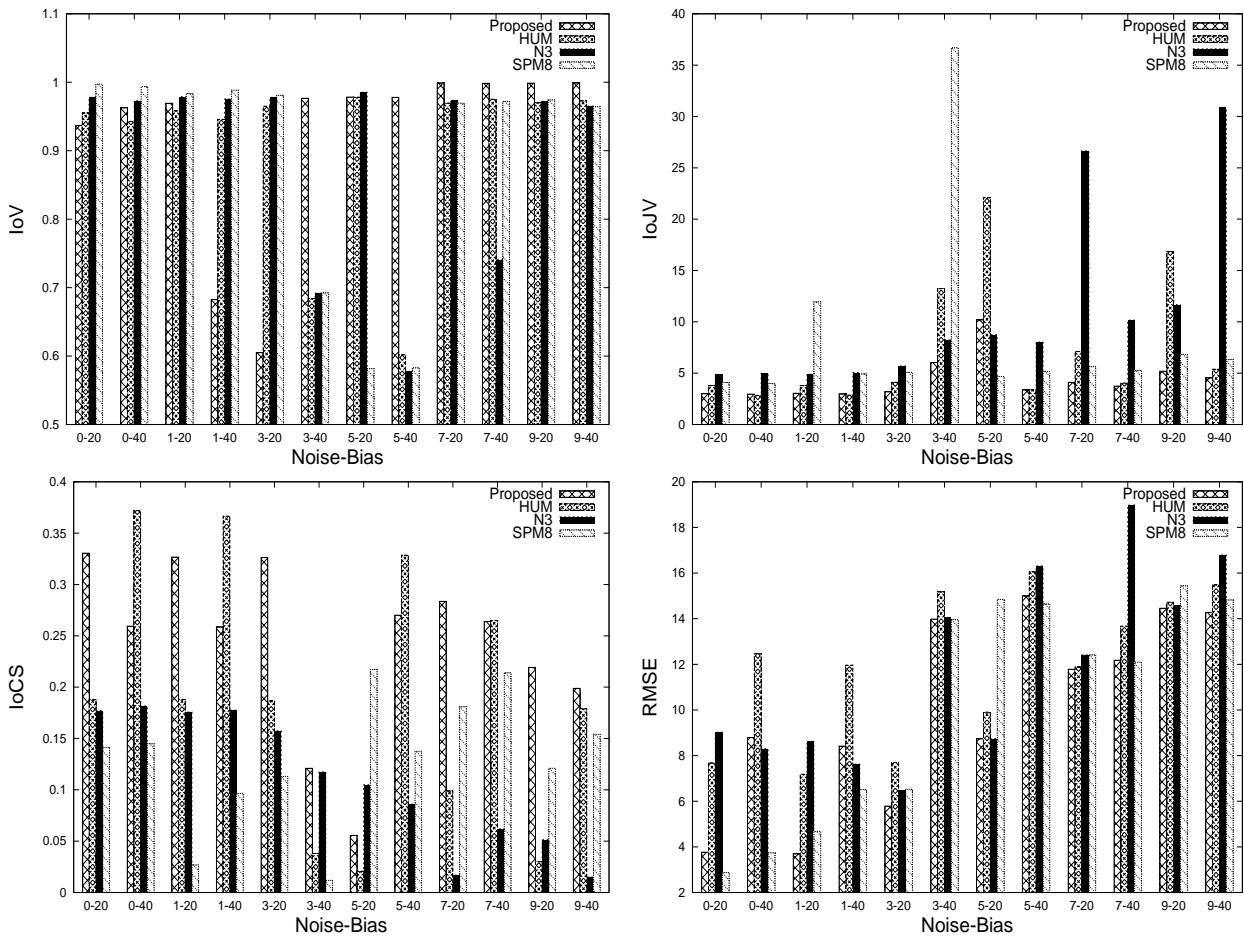


Fig. 23. Comparative performance of the proposed method, HUM algorithm of Brinkmann et al., N3 bias correction algorithm and SPM8 software tool for bias affected images from BrainWeb database

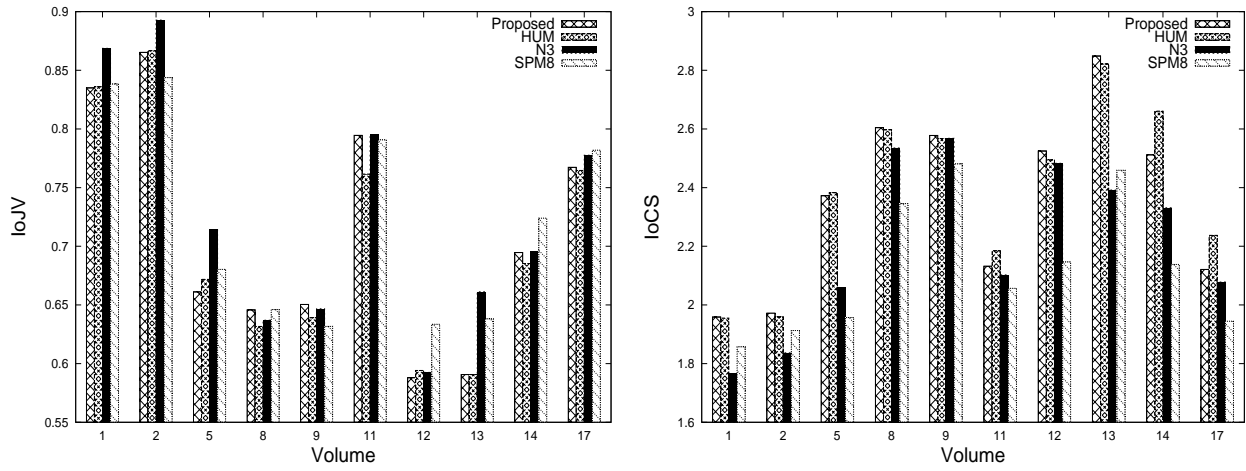


Fig. 24. Comparative performance of the proposed method, HUM algorithm of Brinkmann et al., N3 bias correction algorithm and SPM8 software tool for bias affected images from IBSR database

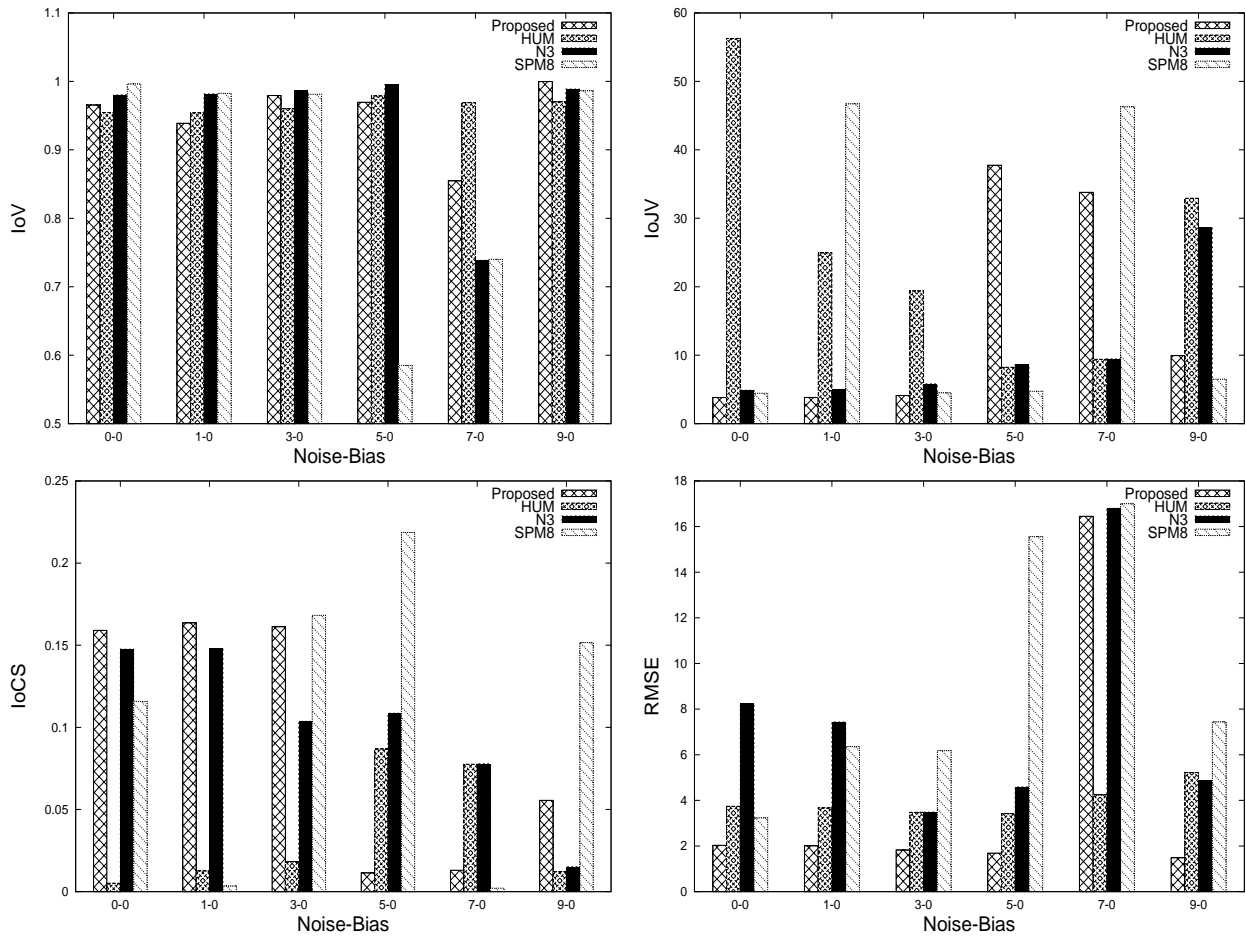


Fig. 25. Comparative performance of the proposed method, HUM algorithm of Brinkmann et al., N3 bias correction algorithm and SPM8 software tool for unbiased images from BrainWeb database

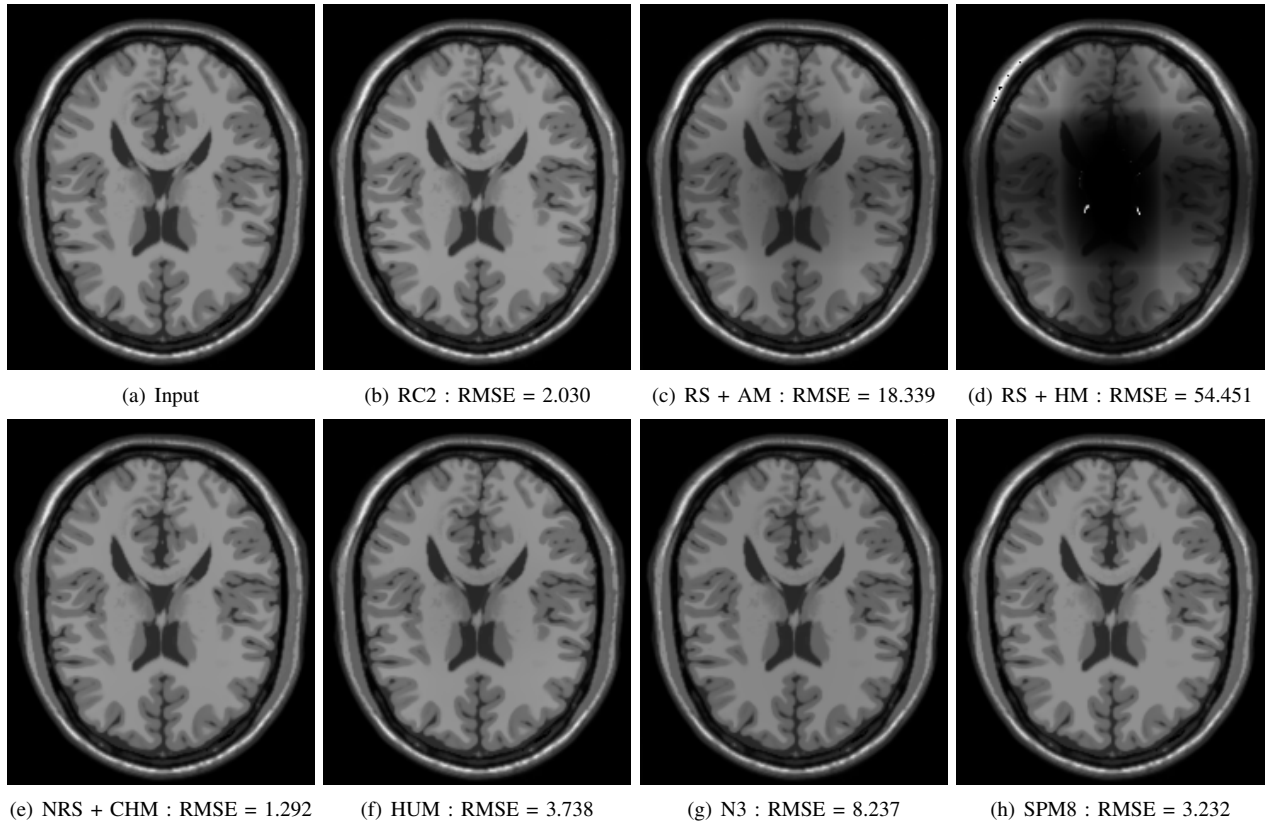


Fig. 26. Image of BrainWeb with 0% bias field and 0% noise and images restored by different algorithms

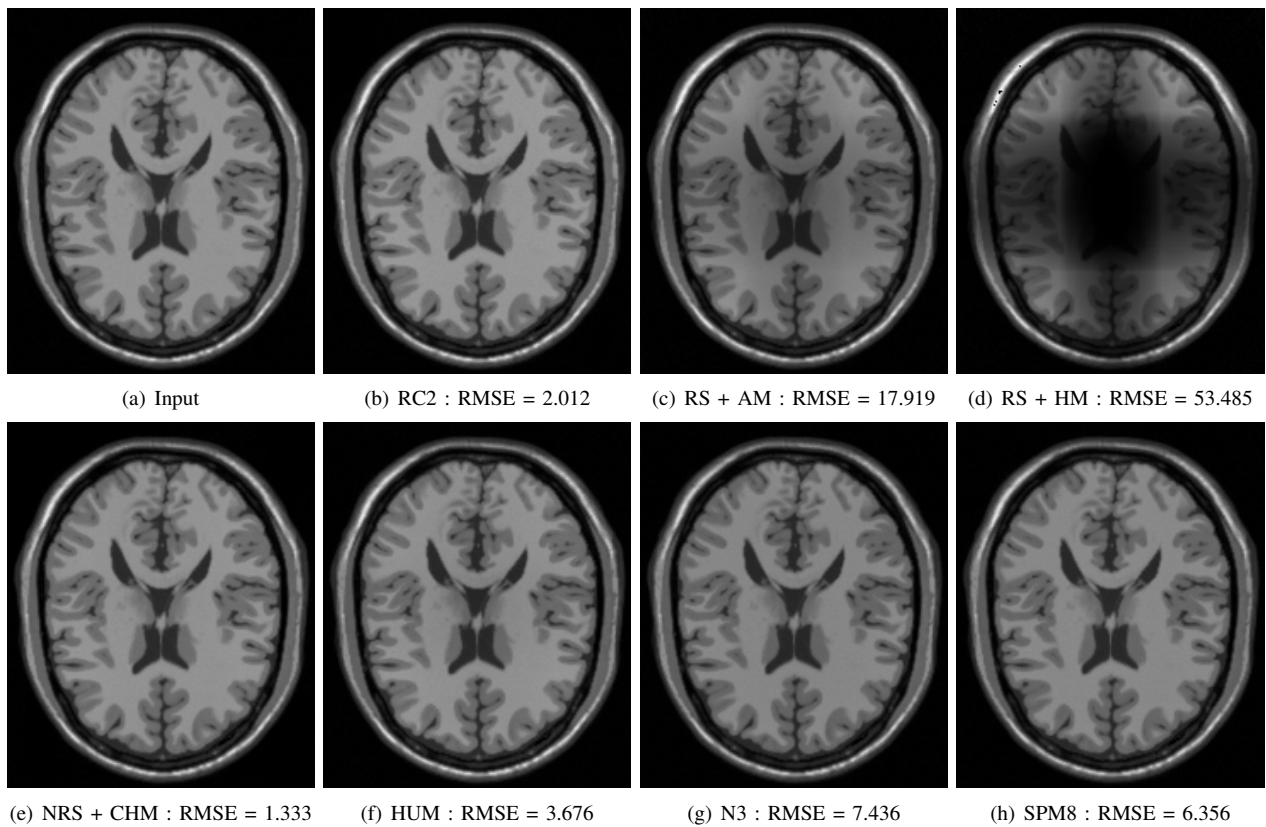


Fig. 27. Image of BrainWeb with 0% bias field and 1% noise and images restored by different algorithms

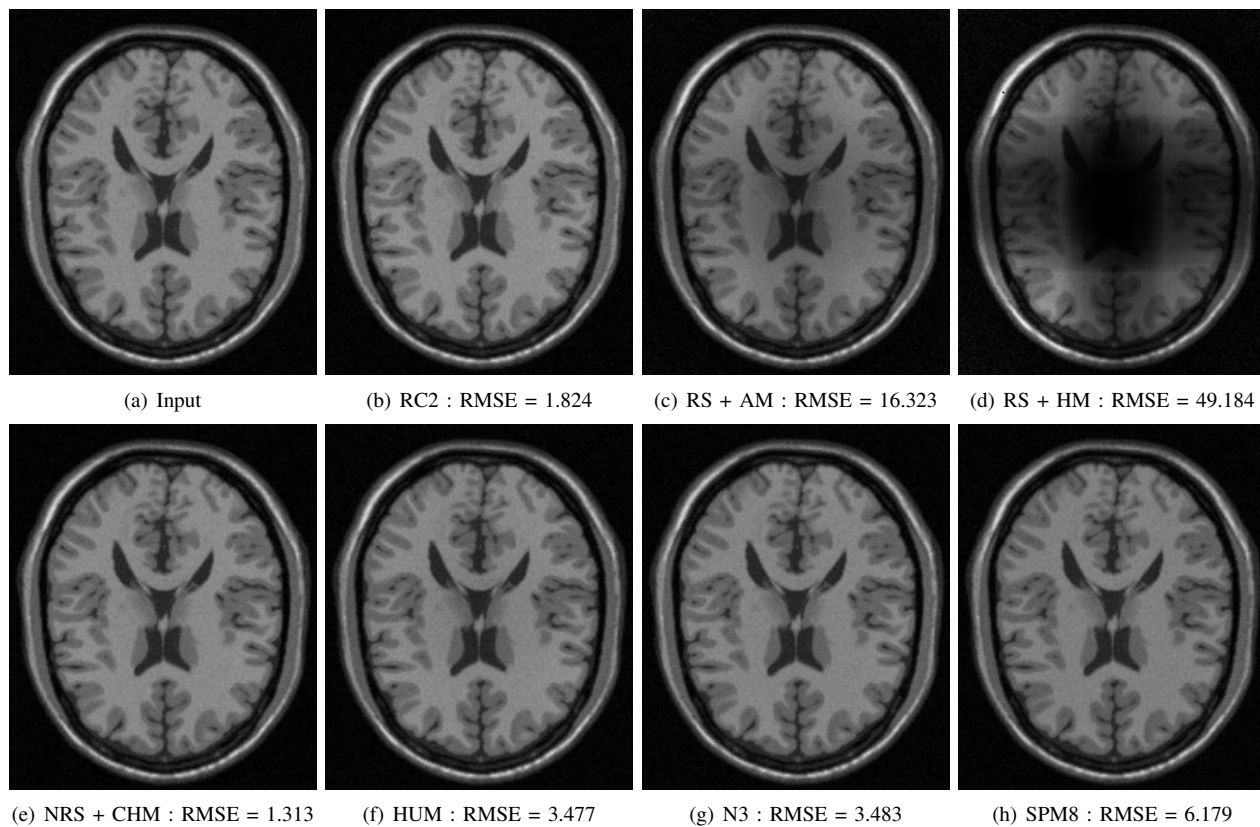


Fig. 28. Image of BrainWeb with 0% bias field and 3% noise and images restored by different algorithms

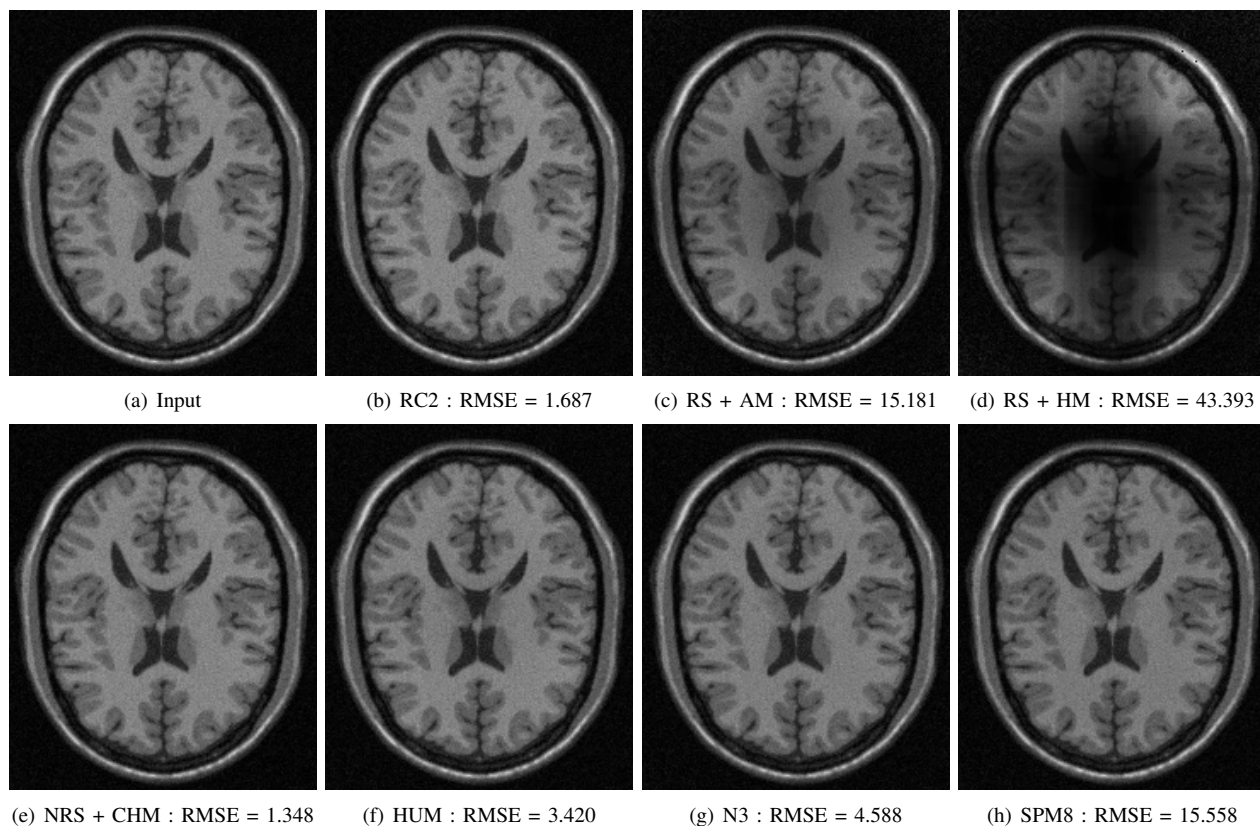


Fig. 29. Image of BrainWeb with 0% bias field and 5% noise and images restored by different algorithms

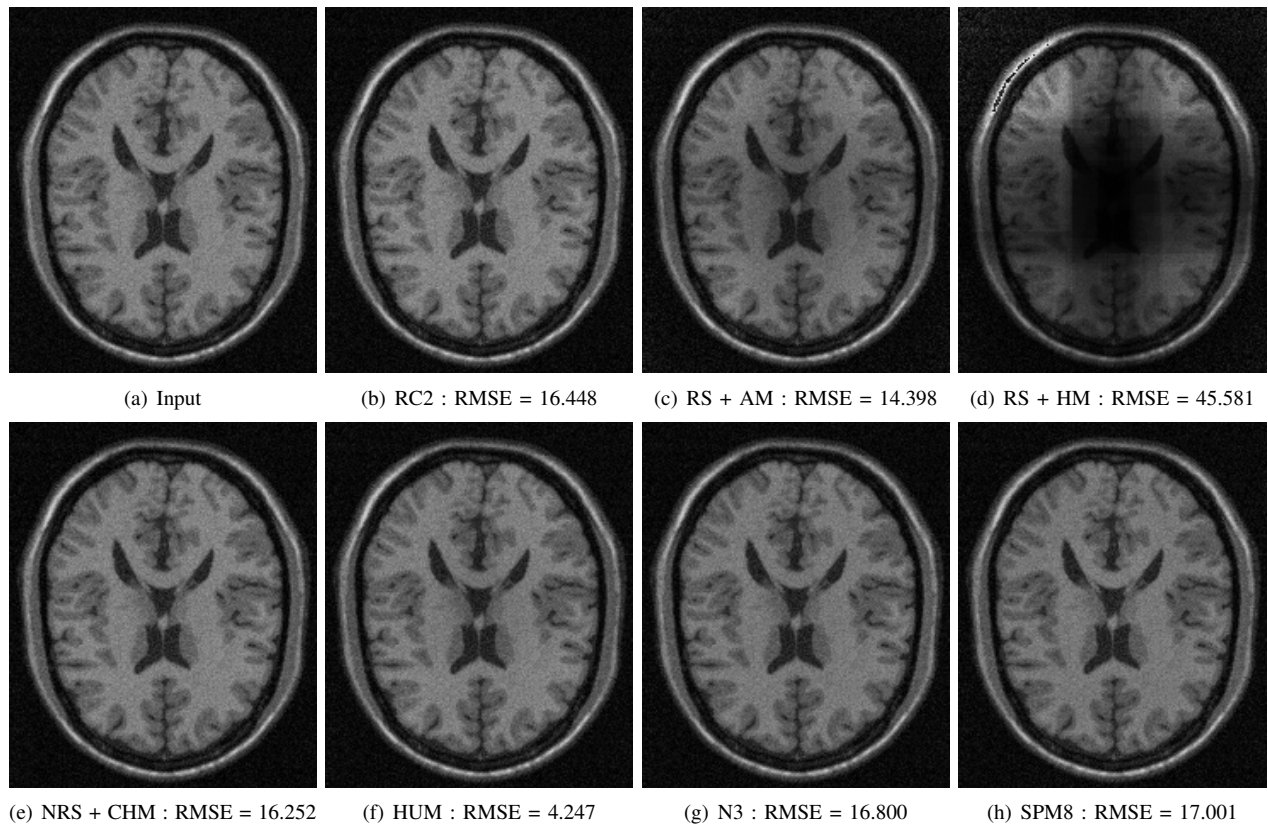


Fig. 30. Image of BrainWeb with 0% bias field and 7% noise and images restored by different algorithms

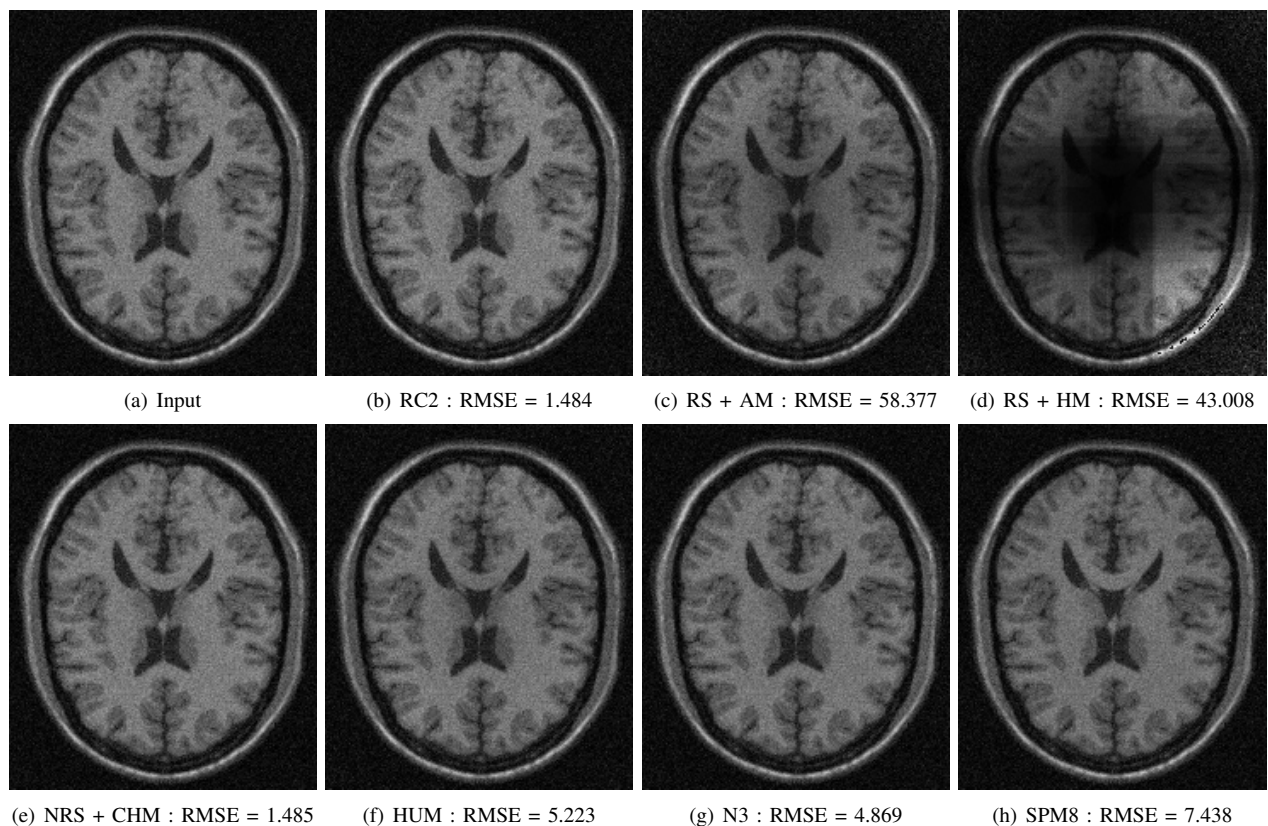


Fig. 31. Image of BrainWeb with 0% bias field and 9% noise and images restored by different algorithms